

Blue-to-UVB Upconversion, Solvent Sensitization and Challenging Bond Activation Enabled by a Benzene-Based Annihilator

Till J. B. Zähringer, Julian A. Moghtader, Maria-Sophie Bertrams, Bibhisan Roy, Masanori Uji, Nobuhiro Yanai,* and Christoph Kerzig*

Abstract: Several energy-demanding photoreactions require harsh UV light from inefficient light sources. The conversion of low-energy visible light to high-energy singlet states via triplet-triplet annihilation upconversion (TTA-UC) could offer a solution for driving such reactions under mild conditions. We present the first annihilator with an emission maximum in the UVB region that, combined with an organic sensitizer, is suitable for blue-to-UVB upconversion. The annihilator singlet was successfully employed as an energy donor in subsequent FRET activations of aliphatic carbonyls. This hitherto unreported UC-FRET reaction sequence was directly monitored using laser spectroscopy and applied to mechanistic irradiation experiments demonstrating the feasibility of Norrish chemistry. Our results provide clear evidence for a novel blue light-driven substrate or solvent activation strategy, which is important in the context of developing more sustainable light-to-chemical energy conversion systems.

Introduction

Highly energetic photons with wavelengths in the UVB region (280–315 nm) are unavoidably required to initiate numerous useful photochemical reactions^[1,2] and to detoxify many pollutants photochemically.^[3,4] However, two main drawbacks render the broad usage of UVB-driven reactions somewhat cumbersome. Firstly, UVB light is practically not contained in the solar spectrum and the generation of UVB

photons typically requires mercury lamps,^[5] excimer-based lamps,^[6] or the high-energy tail of xenon arc lamps^[4]—all of them suffer from rather short lifespans well below 2000 h and electricity-to-UVB conversion efficiencies close to zero. Secondly, conventional glassware used in chemical laboratories has a low UVB transparency, which is why more expensive quartz glass is required for conventional UVB photochemistry.

In principle, the energy of two visible photons efficiently generated by long-lived LEDs can be pooled to achieve similar reactivities as obtained by direct UVB excitation. Among all known photon pooling or two-photon mechanisms,^[7–11] upconversion via sensitized triplet-triplet annihilation (TTA-UC) provides the most attractive alternative to direct high-energy one-photon excitation, because TTA-UC can be employed to convert two low-energy photons at moderate photon fluxes into one highly energetic singlet-excited state.^[12–23] The latter can either emit one photon of higher energy or directly activate a compound being inert under one-photon conditions at the given excitation wavelength. This strategy has already been exploited for a variety of selective photoreactions upon excitation with inexpensive diode-based continuous wave (cw) light sources,^[24] including isomerizations,^[25–27] dehalogenations,^[28–30] cycloadditions,^[31,32] C–C coupling,^[24,33,34] and cyclization^[30] reactions as well as polymerizations.^[30,35–37] While all these UC-driven reactions are elegant, in particular when red/NIR photons with high penetration depth are used,^[30,38–40] they can likely be initiated by LEDs in a direct manner. Efficient high-power LEDs are available with numerous visible and some UVA (315–400 nm) peak wavelengths, but efficient ready-to-use LEDs with UVB emission do not exist for technical reasons.^[41] Consequently, it is highly desirable to develop visible light-driven UC systems that are capable of producing UVB photons to potentially replace harmful and inefficient light sources.

The first visible light-driven TTA-UC system with pronounced UV emission was reported in 2009.^[42] The interest in this methodology recently received a boost by some applications under remarkably mild conditions and pioneering observations such as the blue-light driven photocatalytic activation of aryl bromides,^[43] water splitting,^[44,45] the quantitative decomposition of a typical water pollutant,^[28] and the development of systems with very high quantum yields for UVA generation.^[46–48] Nevertheless, only a few basic structures for UV annihilators have been identified until now (biphenyl,^[49–51] PPO and strongly related

[*] T. J. B. Zähringer, J. A. Moghtader, M.-S. Bertrams, Prof. Dr. C. Kerzig
Department of Chemistry, Johannes Gutenberg University Mainz
Duesbergweg 10–14, 55128 Mainz (Germany)
E-mail: ckerzig@uni-mainz.de

Dr. B. Roy, M. Uji, Prof. Dr. N. Yanai
Department of Applied Chemistry, Graduate School of Engineering,
Center for Molecular Systems (CMS), Kyushu University
744 Moto-oka, Nishi-ku, Fukuoka 819-0395 (Japan)
E-mail: yanai@mail.cstm.kyushu-u.ac.jp

© 2022 The Authors. Angewandte Chemie International Edition published by Wiley-VCH GmbH. This is an open access article under the terms of the Creative Commons Attribution Non-Commercial License, which permits use, distribution and reproduction in any medium, provided the original work is properly cited and is not used for commercial purposes.

heterocycles,^[42,48,52–54] terphenyl,^[54,55] quarterphenyl,^[55] pyrene^[34,56–58] as well as naphthalene^[28,37,46,51,54,59–61] and all these annihilators mainly show UVA and violet emission with either a negligible fraction of emitted UVB^[62] photons or no UVB emission at all. The identification of an annihilator with dominant UVB emission and the concomitant high excited singlet state energy well beyond 4 eV could expand the toolbox of photochemists drastically, given that Vis-to-UV upconversion holds great promise for energy-demanding photochemical applications.^[63,64] Herein, we present the first compound that deserves the label UVB annihilator: Its emission peaks in the UVB region at 309 nm, about half of the photons emitted via fluorescence lie in the UVB range (Figure 1) and, in combination with a suitable blue light-absorbing sensitizer, blue-to-UV upconversion can be observed with diode-based light sources. The resulting upconversion system was characterized by in-depth mechanistic studies using several spectroscopic techniques and employed for an underexplored upconversion-Förster resonance energy transfer (UC-FRET)^[65,66] reaction sequence. As we will show by meaningful proof-of-concept experiments, this novel strategy can not only be exploited for solvent excitation—a typical approach in synthetic UVB photochemistry^[1,2,6,67]—but also for high-energy carbonyl photochemistry.^[68,69]

Results and Discussion

Chemical intuition suggests that reducing the conjugated π -system from biphenyl to benzene would increase the annihilator's singlet-excited state energy and shift its peak emission from the UVA into the high-energy UVB region. However, the triplet of unsubstituted benzene at 3.9 eV^[70] is inaccessible in blue light-driven upconversion schemes as the input photon energy is on the order of 2.7 eV in this case. Modifications on the annihilator scaffolds with the protection group TIPS-ethynyl (triisopropylsilylethynyl) have shown to lower the triplet energy substantially while

maintaining relatively high energies of the upconverted emission.^[46,50,71–74] Hence, we speculated that benzene would follow a similar trend although previous calculations predicted a very pronounced HOMO–LUMO gap decrease.^[75] Our DFT calculations of several benzene derivatives with different TIPS-ethynyl substitution patterns provided initial information about the triplet energies (Figure 2B, see Section S3 of the Supporting Information for details). While the calculated triplet energies of single-substituted **TIPS-Bz** (3.06 eV) and symmetrical threefold substituted **tTIPS-Bz** (2.97 eV) still exceed our input energy limit, the twofold substitution (**bTIPS-Bz**), however, yielded a rather low triplet energy of 2.57 eV. For that reason, we synthesized **bTIPS-Bz** (and reference compounds) via a Sonogashira coupling reaction (see Supporting Information for details, Section S2). The absorption and normalized emission spectra are shown in Figure 2C. As expected, the two TIPS-ethynyl substituents on benzene cause a red-shift of the absorption and emission peaks (compare Figure S5). Gratifyingly, the emission spectrum of **bTIPS-Bz** peaks in the UVB, about half of all emitted photons are in the UVB range, and its singlet-excited state energy is as high as 4.15 eV, corresponding to a photon energy of 299 nm. Owing to the superincrease of the molar absorptivity (Figure S5), the fluorescence rate constant of **bTIPS-Bz** is increased drastically compared to that of benzene.^[76–78] In direct consequence, (i) the fluorescence lifetime in solution (Figure S14) is shortened from 30 ns (benzene) to 3.2 ns (**bTIPS-Bz**) and (ii) the fluorescence quantum yield reaches an attractive value of $\Phi_{\text{Fl}}=0.48$ for **bTIPS-Bz**, compared to $\Phi_{\text{Fl}}=0.07$ for benzene.^[79,80] From 77 K phosphorescence measurements, we obtained a triplet energy of 2.64 eV for **bTIPS-Bz** (Figure S17), which is in very good agreement

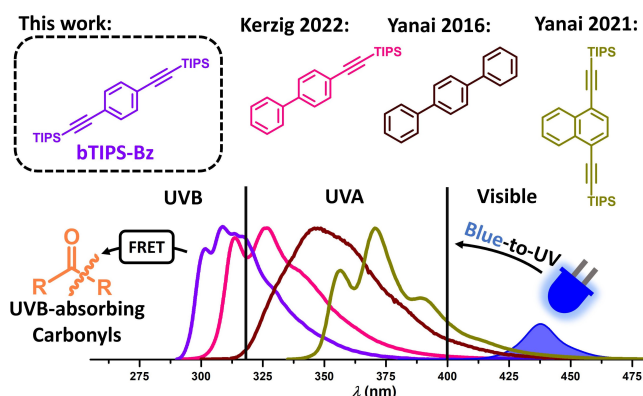


Figure 1. Structures and emission spectra of recently used annihilators for blue-to-UV upconversion. This work: Novel benzene-based annihilator (**bTIPS-Bz**) suitable for blue-to-UV upconversion that has been successfully employed as an energy donor in a subsequent FRET activation of UVB-absorbing carbonyls.

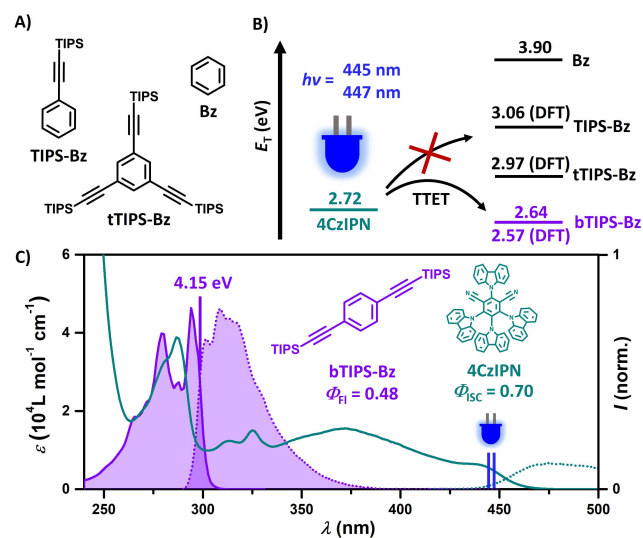


Figure 2. A) Structures of **TIPS-Bz**, **tTIPS-Bz** and **Bz**. B) Energy diagram visualizing the lowest triplet-excited state energies of **4CzIPN**, unsubstituted benzene, and TIPS-ethynyl substituted benzenes. C) Structures, absorption (solid line), and normalized emission (dotted line) spectra of **bTIPS-Bz** and **4CzIPN** in cyclohexane. The excitation wavelengths (445 nm and 447 nm) used for upconversion measurements are indicated by blue vertical lines.

with that estimated by DFT calculations. Given that isoenergetic and even slightly uphill sensitization is feasible,^[31,81–83] TTA-UC with **bTIPS-Bz** as annihilator is clearly within reach using blue photons.

For this study, we have chosen the well-known carbazolyl dicyanobenzene-based TADF emitter **4CzIPN** (Figure 2B and C) as the triplet sensitizer. In addition to OLED applications,^[84] **4CzIPN** has been successfully employed in energy transfer catalysis^[85,86] and TTA-UC schemes.^[50,55,87] Its high triplet energy (2.72 eV in cyclohexane), high triplet formation yield (about 70%)^[88] and strong absorptivity in the blue make it ideal for our blue light-driven upconversion system.^[50] For solubility reasons, toluene was used as co-solvent (10 vol.%), which does not negatively affect the pertinent properties of our photoactive compounds (see ref. [50] and Figures S6/S14). The combined key properties of both **4CzIPN** and **bTIPS-Bz** are summarized in Figures 2B and C. Transient absorption (TA) and emission spectroscopy using laser flash photolysis (LFP) were performed with a 355 nm laser (≈ 5 ns pulse duration) to investigate the upconversion system in detail. The initial energy transfer from $^3\text{4CzIPN}$ to **bTIPS-Bz** proceeds with a quenching rate constant of $k_{\text{TTET}} = 6.2 \times 10^7 \text{ M}^{-1} \text{ s}^{-1}$ (Figure 3A), which is not only in line with the rather small triplet energy difference between $^3\text{bTIPS-Bz}$ and $^3\text{4CzIPN}$

but also sufficiently rapid for efficient quenching ($> 85\%$) of $^3\text{4CzIPN}$ at moderate concentrations ($> 9 \text{ mM}$). In contrast, no quenching of the other TIPS-ethynyl substituted benzenes—**TIPS-Bz** and **tTIPS-Bz**—was observed, highlighting the unique photochemical properties of **bTIPS-Bz**. Further TA measurements were carried out to monitor the quenching product. The $^3\text{4CzIPN}$ quenching by **bTIPS-Bz** gave rise to a TA spectrum with a pronounced absorption band peaking at 348 nm (purple spectrum in Figure 3B) that completely returns to baseline (Figure S18) with wavelength-independent kinetics and a much longer lifetime ($\approx 120 \mu\text{s}$) compared to $^3\text{4CzIPN}$ alone (7.9 μs , see Figure S12 and corresponding discussion for further explanations). TD-DFT calculations on $^3\text{bTIPS-Bz}$ predict an intense absorption peak at 360 nm matching our experiments well (see calculated transitions in Figure 3B and Section S3 of the Supporting Information for details). We, therefore, assign the spectrum displayed in Figure 3B (purple) to $^3\text{bTIPS-Bz}$ generated through triplet-triplet energy transfer TTET.

Having established sensitized annihilator triplet formation, we next examined the TTA step. Three solutions containing either **bTIPS-Bz**, **4CzIPN**, or both in combination were prepared and investigated using time-gated emission spectroscopy. The detection window after 355 nm excitation was selected such that direct sensitizer and annihilator emission can be excluded. Out of the three solutions, only that with **4CzIPN** and **bTIPS-Bz** shows the expected singlet emission in the UV (Figure 3C) providing evidence for delayed annihilator emission, which has to be a result of TTA. The similar triplet energies imply the possibility of back-energy transfer in the triplet manifold. Kinetic emission traces monitoring delayed $^1\text{bTIPS-Bz}^*$ emission at 319 nm with increasing sensitizer concentration confirm a back-TTET (Figure 3C, inset), as indicated by the delayed emission lifetime decrease.^[28,89,90] Moreover, we observed that the triplet lifetime of $^3\text{bTIPS-Bz}$ correlates with the weak elongated **4CzIPN** emission from back-TTET (Figure S13), and we attribute the remaining spectral emission of **4CzIPN** in Figure 3C to this energy transfer equilibrium.^[50,89]

More direct evidence for the UV emission originating from TTA-UC is given in Figure 3D. Kinetic traces simultaneously monitoring $^3\text{bTIPS-Bz}$ (absorption at 342 nm) and $^1\text{bTIPS-Bz}^*$ (emission at 319 nm) show that both reach a maximum at $t = 6 \mu\text{s}$. Owing to the bimolecular nature of the annihilation process, the rise and fall of the singlet emission intensity are in a quadratic relation to the triplet concentration [$^3\text{bTIPS-Bz}$], resulting in the characteristic behavior displayed in Figure 3D.^[91] We then characterized the efficiency of this novel blue-to-UVB TTA-UC scheme with two blue diode-based cw lasers at either 447 nm or 445 nm (see Supporting Information for detailed descriptions of both setups). We found that a sensitizer concentration of $44 \mu\text{M}$ gave a good compromise between the overall quantum yield and the threshold intensity I_{th} . Although higher sensitizer concentrations are regarded to be beneficial for lowering I_{th} ,^[92] i.e., for achieving high quantum yields at low light intensities, we found a higher I_{th} at $88 \mu\text{M}$ (see

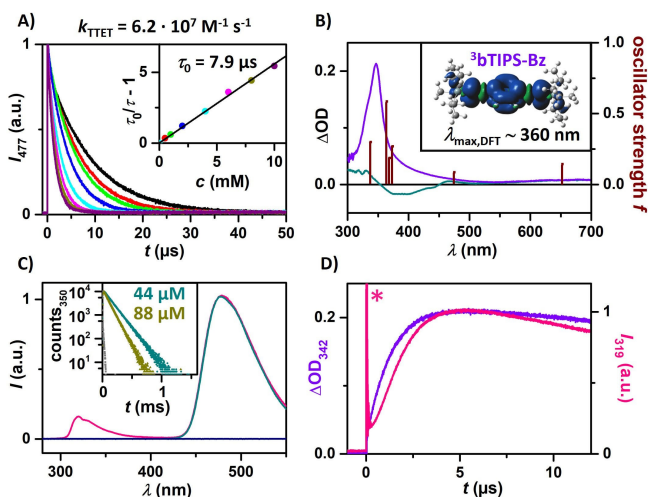


Figure 3. Mechanistic LFP experiments with 355 nm laser pulses of ≈ 5 ns duration. If not stated otherwise $20 \mu\text{M}$ **4CzIPN** and 10 mM **bTIPS-Bz** in Ar-saturated cyclohexane:toluene (9:1) were used. A) Luminescence quenching experiments of **4CzIPN** (detection wavelength, 477 nm) at different annihilator concentrations. Inset: corresponding Stern–Volmer plot. B) Transient absorption spectra of only **4CzIPN** (cyan) recorded $1 \mu\text{s}$ after the laser pulse and combined with **bTIPS-Bz** after $6 \mu\text{s}$ (purple) and oscillator strength of $^3\text{bTIPS-Bz}$ computed by TD-DFT. Inset: Computed spin density of the triplet state of **bTIPS-Bz** with $\lambda_{\text{max,DFT}}$ of the predicted main absorption bands. C) Normalized time-gated (delay, $6 \mu\text{s}$; integration over $500 \mu\text{s}$) emission spectra of the complete upconversion system (pink), only **4CzIPN** (cyan), and only **bTIPS-Bz** (dark blue). Inset: Time-resolved upconversion emission plotted logarithmically at different sensitizer concentrations under pulsed excitation at 445 nm . D) Time-resolved emission (319 nm) and transient absorption (342 nm) traces upon excitation of the UC system. The asterisk marks laser stray light.

Figure S7). This observation is most likely a result of back-TTET with sensitizer ground state molecules as an additional deactivation pathway of the annihilator triplet.

The main plot in Figure 4A collates the upconverted emission with increasing laser intensity (10–800 mW) peaking at 318 nm with intense emission in the UVB region. The higher annihilator concentration causes filter effects of the annihilator emission in its absorption-emission overlap region (compare spectra in Figures 2C and 4A), thereby shifting the apparent emission maximum. However, the absorption of the ¹bTIPS-Bz*-emitted photons by additives in solution could occur below 310 nm—it would simply compete with annihilator self-absorption. Using the observed UC emission maximum in combination with the absorption maximum of 4CzIPN (435 nm), the anti-Stokes shift amounts to 1.04 eV.^[16] A frequently employed but less conservative anti-Stokes shift determination would yield a value as high as 1.24 eV, taking the excitation wavelength (447 nm) and the bTIPS-Bz emission peak in the absence of inner filter effects (309 nm). Regardless of the actual method, the anti-Stokes shift of our system is among the largest reported so far for visible light-driven UC schemes.^[72,82,93–100]

Figures 4B and C focus on power-dependent UC measurements. The achievable upconversion quantum yields Φ_{UC} at the highest laser intensities amount to values close to 1% (with a theoretical maximum of 50%) using both 447 nm and 445 nm excitation. A rather low I_{th} of 471 mW cm⁻² was determined (using the 445 nm setup with higher beam

quality), enabling decent UC efficiencies already with commercially available blue LEDs (Figure S15). Moreover, irradiating the UC system at the threshold intensity shows only minor degradation over one hour (Figure 4A, inset). Higher sensitizer concentrations (88 μ M) seem to be beneficial for the photostability of this system. A more systematic understanding of the factors governing efficient upconversion into the UV region seems to be required, considering the typically poor performance parameters of most known Vis-to-UV UC systems.^[49,101] The most straightforward future strategies for developing Vis-to-UVB UC systems with higher overall quantum yields are to increase the annihilator emission quantum yield (48%) by up to a factor of two and to avoid back-TTET with sensitizers possessing higher tripler energies that could also result in UC systems operating at lower annihilator concentrations (i.e., with less pronounced filter effects). Nevertheless, the promising efficiency and long-term stability led us to speculate that our unprecedented UC system with pronounced UVB emission could perhaps drive energy-demanding reactions that usually require high-energy UVB light sources, either with the singlet-excited annihilator as reacting key species or via an emission-reabsorption sequence.^[102]

We proposed that the high singlet-excited state energy of bTIPS-Bz could be exploited for a subsequent FRET activation of relatively inert substances (Figure 5A) with a rich UV photochemistry. UC-FRET reaction sequences have been suggested with less energetic excited states of the energy acceptor that would be accessible with efficient LEDs,^[65,66,103] but in our high-energy case, such an alternative does not exist. For our study, we chose pinacolone (PC) and acetone (AC)—both absorb only below 320 nm and thus usually require harmful UVB light sources for excitation. Figure 5B visualizes the spectral overlap between the bTIPS-Bz emission and the absorption of the carbonyl compounds. Although the molar absorption coefficients of such aliphatic carbonyls are rather low due to the symmetry-forbidden nature of the $n\pi^*$ transitions, the pronounced spectral overlap suggests that non-radiative energy transfer via the FRET mechanism is still feasible, whose efficiency linearly depends on the spectral overlap integrals.^[104] NMR-scale and mechanistic LFP experiments were conducted to monitor the UC-FRET sequence. Figure 5E shows kinetic traces of the bTIPS-Bz emission at 318 nm with increasing PC and AC concentrations. While the formation and decay rates of the singlet emission signals are essentially unaffected by the addition of the carbonyl compound, the overall emission intensity is reduced drastically. This contrasts strongly with time-resolved measurements of the bTIPS-Bz triplet state where no change with the addition of PC or AC (neither in concentration nor in lifetime) is observed (Figure S8). Thus, the initial amount of ¹bTIPS-Bz* produced via annihilation has to be unaffected by the addition of the carbonyls and we conclude that the attenuated UC emission signal must originate from direct excited-singlet state quenching^[43] (most likely via FRET) or reabsorption effects. An estimation of the latter, i.e., reabsorbed photons by the carbonyls through radiative energy transfer, revealed that non-radiative excited state quenching is the main pathway at

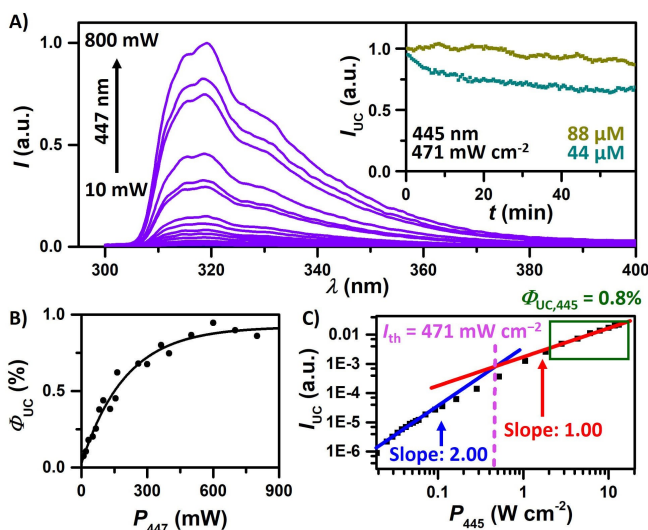


Figure 4. Photon upconversion studies with deoxygenated solutions containing 44 or 88 μ M 4CzIPN and 10 mM bTIPS-Bz in cyclohexane: toluene (9:1) using a cw laser for excitation at 447 nm or 445 nm. A) Power-dependent spectra of the normalized upconverted emission. Inset: Photostability measurement at different sensitizer concentrations at a cw laser power of 471 mW cm⁻². B) External upconversion quantum yield, Φ_{UC} , plotted against the laser power (with 44 μ M 4CzIPN). C) Normalized UC emission plotted against the laser power on a double-logarithmic scale (with 44 μ M 4CzIPN). The threshold intensity I_{th} was determined from the crossing point. See Supporting Information for details.

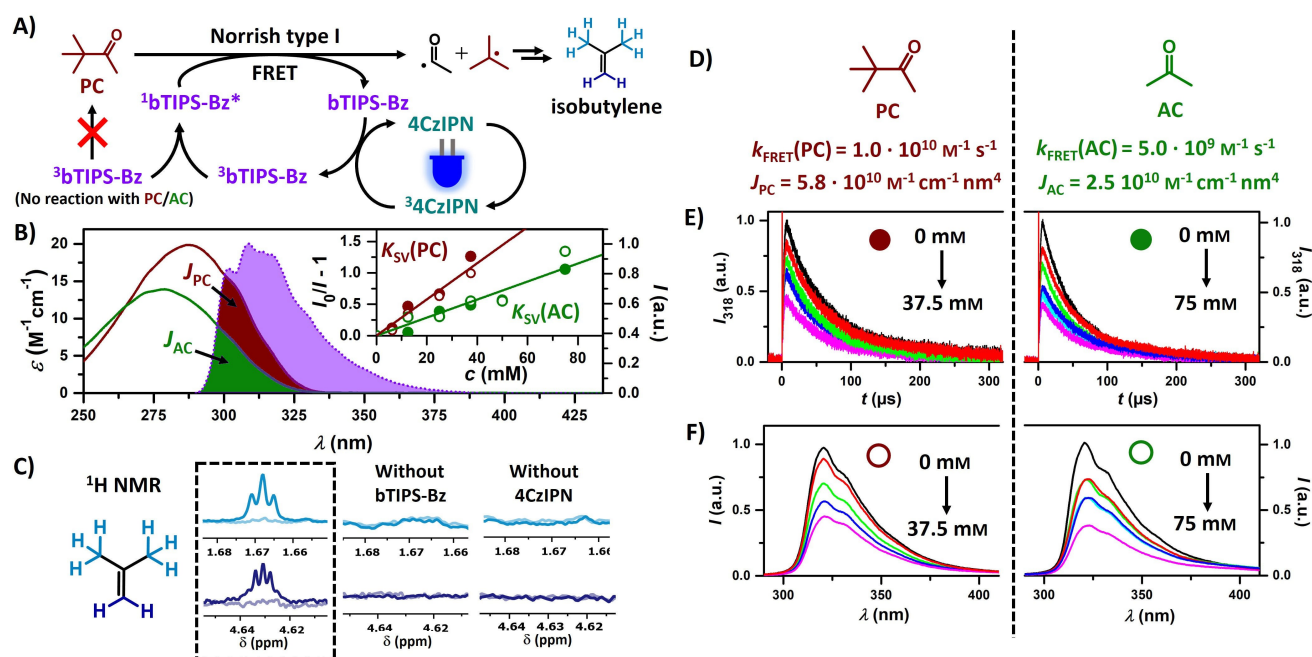


Figure 5. A) Upconversion mechanism and subsequent FRET sensitization of pinacolone resulting in a Norrish type I reaction and formation of isobutylene. B) Absorption spectra (solid line) of pinacolone (dark red), acetone (green), and normalized emission (dotted line) of **bTIPS-Bz** in cyclohexane with the spectral overlap being highlighted. Inset: Stern–Volmer plot corresponding to quenching of upconverted **bTIPS-Bz** emission by the carbonyl compounds. C) NMR scale experiment of 100 μM **4CzIPN**, 10 mM **bTIPS-Bz**, and 100 mM pinacolone in Ar-saturated cyclohexane: toluene (9:1) with control experiments before and after 30 min irradiation at 447 nm with 1.1 W. Shown are the ^1H NMR signals of isobutylene as a stable product of the UC-FRET-driven Norrish reaction. D) Comparison of FRET efficiencies between pinacolone and acetone. E) and F) Mechanistic LFP experiments with 355 nm laser pulses of ≈ 10 ns duration of 20 μM **4CzIPN** and 10 mM **bTIPS-Bz** in Ar-saturated cyclohexane: toluene (9:1) with different concentrations of pinacolone and acetone used for the Stern–Volmer plots in the inset of panel B). E) Time-resolved emission at 318 nm. F) Normalized time-gated (delay, 6 μs ; integration over 500 μs) emission spectra.

our detection wavelength used in Figure 5E (see Supporting Information Section S6). Further time-gated spectra of the UV emission yielded a very similar decrease in intensity (Figure 5F). Moreover, the signal intensity in the region above 330 nm (where the carbonyls do not absorb) is almost equally reduced compared to the emission peak (318 nm) (Figure S9). All these findings are in perfect accordance with a FRET process between $^1\text{bTIPS-Bz}^*$ and the carbonyls being the main quenching mechanism of the upconverted emission. Similar quenching experiments were also performed with a cw laser (447 nm) to demonstrate the feasibility of this energy transfer sequence with a non-pulsed visible light source (Figure S10). Next, we investigated the energy transfer efficiency in detail. In principle FRET is still feasible at larger molecular distances (up to 100 nm), meaning that the energy transfer rate can exceed the classical diffusion limit for collision-induced quenching. As a result of the low molar absorption coefficients of the carbonyls, we pre-calculated rather small Förster distances of 0.7 nm and 0.8 nm for **AC** and **PC** (Section S1.8 of the Supporting Information), suggesting that the quenching constant will be close to or slightly higher than the diffusion-controlled rate constant in cyclohexane ($k_{\text{diff}} = 6.7 \times 10^9 \text{ M}^{-1} \text{ s}^{-1}$).^[105] The $^1\text{bTIPS-Bz}^*$ emission intensity from either kinetic measurements (filled circle, raw data from Figure 5E) or time-gated spectra (open circle, raw data from Figure 5F) are plotted against the carbonyl concentration in a Stern–Volmer graph

(Figure 5B, inset). Conventional Stern–Volmer analyses gave quenching constants k_{FRET} of $5.0 \times 10^9 \text{ M}^{-1} \text{ s}^{-1}$ for **AC** and $1.0 \times 10^{10} \text{ M}^{-1} \text{ s}^{-1}$ for **PC**, respectively (Figure 5D). Direct fluorescence lifetime quenching experiments upon UVB excitation of **bTIPS-Bz** with different acetone concentrations gave a similar result ($k_{\text{FRET}} = 6.4 \times 10^9 \text{ M}^{-1} \text{ s}^{-1}$, see Figure S11 and corresponding discussion in the Supporting Information). The ratios of the energy transfer rate constants and the corresponding spectral overlap integrals J_{PC} and J_{AC} are practically identical, providing further evidence for the novel blue-to-UVB UC-FRET reaction sequence. Efficient photoredox reactions between the high-energy annihilator singlet and the carbonyl compounds or the sensitizer itself can be excluded as we could not detect any signatures of radical ions (Figures S8 and S18 in the Supporting Information).

The diverse photochemistry of carbonyl compounds is well described in the literature.^[1,2,67–69] Acetone almost quantitatively produces a highly energetic triplet state (triplet energy, ≈ 3.5 eV) upon direct excitation, which explains its dual use as solvent and sensitizer in conventional UVB photoreactions. Monitoring the acetone triplet produced via UC-FRET by spectroscopic methods is very challenging owing to its rather slow formation and the relatively high concentrations of potential triplet energy acceptors in our system. However, pinacolone undergoes efficient Norrish type I fragmentation generating a more

stabilized carbon-centered radical (Figure 5A)^[106] compared to that formed by acetone. This isobutyl radical is hard to track spectroscopically, but isobutylene as its stable disproportionation product^[107] (Figure 5A) is sufficiently soluble in our mixture and possesses a characteristic ¹H NMR spectrum.^[108] We, therefore, performed several NMR-scale irradiation experiments with **PC**. Irradiating the whole UC system together with 100 mM **PC** using our cw laser (447 nm) for 30 min resulted in the formation of new peaks in the NMR spectrum that unambiguously correspond to isobutylene (Figure 5C, see Section S8.2 for details). Control experiments with either annihilator or sensitizer missing did not show any evidence for product generation. To demonstrate that this high-energy Norrish chemistry is also viable with commercial blue LEDs, the same irradiation experiment was carried out with two blue LEDs (440 nm). Similar amounts of isobutylene were detected (Figure S29), confirming the promising performance parameters and the potential of our UC system for future lab-scale applications without UVB lamps.

Finally, we turned to the substrate dibenzyl ketone, which is known to undergo efficient Norrish fragmentation under UV photolysis ($\lambda < 325$ nm) and subsequent C–C bond formation of the resulting radicals.^[69] The coupling product dibenzyl has been observed clearly employing our UC-FRET strategy with blue LEDs (Figures S31–S33). This coupling reaction under mercury-free and very mild conditions highlights that more synthetically useful photoreactions are generally feasible employing our new approach.

Conclusion

In summary, we have demonstrated that UVB emitters can be incorporated in blue light-driven upconversion schemes. Reaching the UVB region with blue input photons for the first time is certainly beyond a pushing-the-limits study because this technology enables unreported substrate and solvent activation strategies that cannot be carried out with efficient and sustainable light sources in a direct manner. Our mechanistic investigations provide unambiguous evidence for a hitherto unreported blue-to-UVB UC-FRET sequence expanding the applicability of upconversion for driving challenging chemical reactions. These key findings pave the way for exploiting the full potential of this attractive two-photon mechanism in light-driven bond activation. The incorporation of such high-energy upconversion systems in solid or gel-like environments for large-scale applications might represent the next challenge and even LED-driven UVA-to-UVC upconversion systems, which have the potential to replace mercury lamps completely, seem to be within reach based on our results. The latter would require further efforts in developing both novel annihilators and energy-matched sensitizers that are highly photostable. For that, a deeper understanding of TTA^[73,109–112] is required, and regarding sensitizer development, the upconversion community will strongly benefit from the recent progress in Dexter energy transfer catalysis.^[49,113–116]

Acknowledgements

We acknowledge generous financial support from the JGU Mainz, SusInnoScience, the German Research Foundation (DFG, grant number KE 2313/3-1), the German Federal Environmental Foundation (DBU, PhD fellowship to T.J.B.Z., grant number 20022/028), the Murata Science Foundation, Research Foundation for Opto-Science and Technology and JSPS KAKENHI (JP20H02713, JP22K19051, JP22F21031). C.K. is grateful to the Chemical Industry Funds for a Liebig fellowship. B.R. acknowledges JSPS for a fellowship to conduct research in Japan (P21031). We thank Johannes Rocker for recording mass spectra and Prof. Till Opatz for allowing us to use his equipment. Open Access funding enabled and organized by Projekt DEAL.

Conflict of Interest

The authors declare no conflict of interest.

Data Availability Statement

The data that support the findings of this study are available in the Supporting Information of this article. The raw data sets presented in the main manuscript can be found under <http://doi.org/10.25358/openscience-8436>.

Keywords: Energy Transfer • Photochemistry • Sustainable Chemistry • Time-Resolved Spectroscopy • Upconversion

- [1] P. Klán, J. Wirz, *Photochemistry of Organic Compounds: From Concepts to Practice*, Wiley, Chichester, **2009**.
- [2] N. Hoffmann, *Chem. Rev.* **2008**, *108*, 1052–1103.
- [3] G. S. Pozan, A. Kambur, *Appl. Catal. B* **2013**, *129*, 409–415.
- [4] N. Zhang, G. Liu, H. Liu, Y. Wang, Z. He, G. Wang, *J. Hazard. Mater.* **2011**, *192*, 411–418.
- [5] O. Shvydkiv, S. Gallagher, K. Nolan, M. Oelgemöller, *Org. Lett.* **2010**, *12*, 5170–5173.
- [6] A. G. Griesbeck, N. Maptue, S. Bondock, M. Oelgemöller, *Photochem. Photobiol. Sci.* **2003**, *2*, 450–451.
- [7] F. Glaser, C. Kerzig, O. S. Wenger, *Angew. Chem. Int. Ed.* **2020**, *59*, 10266–10284; *Angew. Chem.* **2020**, *132*, 10350–10370.
- [8] J. Castellanos-Soriano, J. C. Herrera-Luna, D. Díaz Díaz, M. C. Jiménez, R. Pérez-Ruiz, *Org. Chem. Front.* **2020**, *7*, 1709–1716.
- [9] Y. Kobayashi, J. Abe, *Chem. Soc. Rev.* **2022**, *51*, 2397–2415.
- [10] I. Ghosh, L. Marzo, A. Das, R. Shaikh, B. König, *Acc. Chem. Res.* **2016**, *49*, 1566–1577.
- [11] M. Cybularczyk-Cecotka, J. Szczepanik, M. Giedyk, *Nat. Catal.* **2020**, *3*, 872–886.
- [12] V. Gray, D. Dzebo, M. Abrahamsson, B. Albinsson, K. Moth-Poulsen, *Phys. Chem. Chem. Phys.* **2014**, *16*, 10345–10352.
- [13] J. Zhao, S. Ji, H. Guo, *RSC Adv.* **2011**, *1*, 937–950.
- [14] T. N. Singh-Rachford, F. N. Castellano, *Coord. Chem. Rev.* **2010**, *254*, 2560–2573.
- [15] T. F. Schulze, T. W. Schmidt, *Energy Environ. Sci.* **2015**, *8*, 103–125.
- [16] Y. Zhou, F. N. Castellano, T. W. Schmidt, K. Hanson, *ACS Energy Lett.* **2020**, *5*, 2322–2326.

- [17] Z. Xu, Z. Huang, T. Jin, T. Lian, M. L. Tang, *Acc. Chem. Res.* **2021**, *54*, 70–80.
- [18] J. Pedrini, A. Monguzzi, *J. Photonics Energy* **2017**, *8*, 022005.
- [19] L. Zeng, L. Huang, J. Han, G. Han, *Acc. Chem. Res.* **2022**, *55*, 2604–2615.
- [20] T. Lin, C. F. Perkinson, M. A. Baldo, *Adv. Mater.* **2020**, *32*, 1908175.
- [21] H. Liu, X. Yan, L. Shen, Z. Tang, S. Liu, X. Li, *Mater. Horiz.* **2019**, *6*, 990–995.
- [22] S. Balushev, T. Miteva, V. Yakutkin, G. Nelles, A. Yasuda, G. Wegner, *Phys. Rev. Lett.* **2006**, *97*, 143903.
- [23] F. Edhborg, A. Olesund, B. Albinsson, *Photochem. Photobiol. Sci.* **2022**, *21*, 1143–1158.
- [24] R. Pérez-Ruiz, *Top. Curr. Chem.* **2022**, *380*, 23.
- [25] J. B. Bilger, C. Kerzig, C. B. Larsen, O. S. Wenger, *J. Am. Chem. Soc.* **2021**, *143*, 1651–1663.
- [26] Y. Wei, H. Xian, X. Lv, F. Ni, X. Cao, C. Yang, *Mater. Horiz.* **2021**, *8*, 606–611.
- [27] A. Tokunaga, L. M. Uriarte, K. Mutoh, E. Fron, J. Hofkens, M. Sliwa, J. Abe, *J. Am. Chem. Soc.* **2019**, *141*, 17744–17753.
- [28] B. Pfund, D. M. Steffen, M. R. Schreier, M.-S. Bertrams, C. Ye, K. Börjesson, O. S. Wenger, C. Kerzig, *J. Am. Chem. Soc.* **2020**, *142*, 10468–10476.
- [29] C. Kerzig, O. S. Wenger, *Chem. Sci.* **2018**, *9*, 6670–6678.
- [30] B. D. Ravetz, A. B. Pun, E. M. Churchill, D. N. Congreve, T. Rovis, L. M. Campos, *Nature* **2019**, *565*, 343–346.
- [31] C. Wang, F. Reichenauer, W. R. Kitzmann, C. Kerzig, K. Heinze, U. Resch-Genger, *Angew. Chem. Int. Ed.* **2022**, *61*, e202202238; *Angew. Chem.* **2022**, *134*, e202202238.
- [32] R. R. Islangulov, F. N. Castellano, *Angew. Chem. Int. Ed.* **2006**, *45*, 5957–5959; *Angew. Chem.* **2006**, *118*, 6103–6105.
- [33] C. G. López-Calixto, M. Liras, V. A. de la Peña O’Shea, R. Pérez-Ruiz, *Appl. Catal. B* **2018**, *237*, 18–23.
- [34] F. Glaser, C. Kerzig, O. S. Wenger, *Chem. Sci.* **2021**, *12*, 9922–9933.
- [35] N. Awwad, A. T. Bui, E. O. Danilov, F. N. Castellano, *Chem* **2020**, *6*, 3071–3085.
- [36] A. Caron, G. Noirbent, D. Gimes, F. Dumur, J. Lalevée, *Macromol. Rapid Commun.* **2021**, *42*, 2100047.
- [37] Y. Wei, K. Pan, X. Cao, Y. Li, X. Zhou, C. Yang, *CCS Chem.* **2022**, *4*, 3852–3863.
- [38] B. D. Ravetz, N. E. S. Tay, C. L. Joe, M. Sezen-Edmonds, M. A. Schmidt, Y. Tan, J. M. Janey, M. D. Eastgate, T. Rovis, *ACS Cent. Sci.* **2020**, *6*, 2053–2059.
- [39] L. Huang, W. Wu, Y. Li, K. Huang, L. Zeng, W. Lin, G. Han, *J. Am. Chem. Soc.* **2020**, *142*, 18460–18470.
- [40] P. Bharmoria, H. Bildirir, K. Moth-Poulsen, *Chem. Soc. Rev.* **2020**, *49*, 6529–6554.
- [41] H. Hirayama, S. Fujikawa, N. Kamata, *Electron. Commun. Jpn.* **2015**, *98*, 1–8.
- [42] T. N. Singh-Rachford, F. N. Castellano, *J. Phys. Chem. A* **2009**, *113*, 5912–5917.
- [43] M. Majek, U. Faltermeier, B. Dick, R. Pérez-Ruiz, A. Jacobi von Wangelin, *Chem. Eur. J.* **2015**, *21*, 15496–15501.
- [44] A. Monguzzi, A. Oertel, D. Braga, A. Riedinger, D. K. Kim, P. N. Knüsel, A. Bianchi, M. Mauri, R. Simonutti, D. J. Norris, F. Meinardi, *ACS Appl. Mater. Interfaces* **2017**, *9*, 40180–40186.
- [45] M. Barawi, F. Fresno, R. Pérez-Ruiz, V. A. de la Peña O’Shea, *ACS Appl. Energy Mater.* **2019**, *2*, 207–211.
- [46] N. Harada, Y. Sasaki, M. Hosoyamada, N. Kimizuka, N. Yanai, *Angew. Chem. Int. Ed.* **2021**, *60*, 142–147; *Angew. Chem.* **2021**, *133*, 144–149.
- [47] M. Uji, N. Harada, N. Kimizuka, M. Saigo, K. Miyata, K. Onda, N. Yanai, *J. Mater. Chem. C* **2022**, *10*, 4558–4562.
- [48] A. Olesund, J. Johnsson, F. Edhborg, S. Ghasemi, K. Moth-Poulsen, B. Albinsson, *J. Am. Chem. Soc.* **2022**, *144*, 3706–3716.
- [49] L. Schmid, F. Glaser, R. Schaer, O. S. Wenger, *J. Am. Chem. Soc.* **2022**, *144*, 963–976.
- [50] T. J. B. Zähringer, M.-S. Bertrams, C. Kerzig, *J. Mater. Chem. C* **2022**, *10*, 4568–4573.
- [51] X. Lin, Z. Chen, Y. Han, C. Nie, P. Xia, S. He, J. Li, K. Wu, *ACS Energy Lett.* **2022**, *7*, 914–919.
- [52] S. He, X. Luo, X. Liu, Y. Li, K. Wu, *J. Phys. Chem. Lett.* **2019**, *10*, 5036–5040.
- [53] V. Gray, P. Xia, Z. Huang, E. Moses, A. Fast, D. A. Fishman, V. I. Vullev, M. Abrahamsson, K. Moth-Poulsen, M. Lee Tang, *Chem. Sci.* **2017**, *8*, 5488–5496.
- [54] L. Hou, A. Olesund, S. Thurakkal, X. Zhang, B. Albinsson, *Adv. Funct. Mater.* **2021**, *31*, 2106198.
- [55] N. Yanai, M. Kozue, S. Amemori, R. Kabe, C. Adachi, N. Kimizuka, *J. Mater. Chem. C* **2016**, *4*, 6447–6451.
- [56] W. Zhao, F. N. Castellano, *J. Phys. Chem. A* **2006**, *110*, 11440–11445.
- [57] Q. Chen, Y. Liu, X. Guo, J. Peng, S. Garakyaraghi, C. M. Papa, F. N. Castellano, D. Zhao, Y. Ma, *J. Phys. Chem. A* **2018**, *122*, 6673–6682.
- [58] P. Duan, N. Yanai, N. Kimizuka, *Chem. Commun.* **2014**, *50*, 13111–13113.
- [59] Y. Murakami, A. Motooka, R. Enomoto, K. Niimi, A. Kaiho, N. Kiyoyanagi, *Phys. Chem. Chem. Phys.* **2020**, *22*, 27134–27143.
- [60] Z. A. VanOrman, L. Nienhaus, *Matter* **2021**, *4*, 2625–2626.
- [61] J. A. Kübler, B. Pfund, O. S. Wenger, *JACS Au* **2022**, *2*, 2367–2380.
- [62] The only known Vis-to-UV upconversion system with pronounced UVB emission (ref. [49]) requires violet excitation light (405 nm) and operates with quantum yields and threshold intensities that are unattractive for lab-scale applications.
- [63] B. S. Richards, D. Hudry, D. Busko, A. Turshatov, I. A. Howard, *Chem. Rev.* **2021**, *121*, 9165–9195.
- [64] Y. Du, X. Ai, Z. Li, T. Sun, Y. Huang, X. Zeng, X. Chen, F. Rao, F. Wang, *Adv. Photonics Res.* **2021**, *2*, 2000213.
- [65] S. H. C. Askes, M. Kloz, G. Bruylants, J. T. M. Kennis, S. Bonnet, *Phys. Chem. Chem. Phys.* **2015**, *17*, 27380–27390.
- [66] W. Wang, Q. Liu, C. Zhan, A. Barhoumi, T. Yang, R. G. Wylie, P. A. Armstrong, D. S. Kohane, *Nano Lett.* **2015**, *15*, 6332–6338.
- [67] C. Michelin, N. Hoffmann, *ACS Catal.* **2018**, *8*, 12046–12055.
- [68] A. Albini, *Photochem. Photobiol. Sci.* **2021**, *20*, 161–181.
- [69] J. C. Scaiano, K. G. Stamplecoskie, G. L. Hallett-Tapley, *Chem. Commun.* **2012**, *48*, 4798–4808.
- [70] J. P. Doering, *J. Chem. Phys.* **1969**, *51*, 2866–2870.
- [71] P. Bharmoria, F. Edhborg, H. Bildirir, Y. Sasaki, S. Ghasemi, A. Mårtensson, N. Yanai, N. Kimizuka, B. Albinsson, K. Börjesson, K. Moth-Poulsen, *J. Mater. Chem. A* **2022**, *10*, 21279–21290.
- [72] N. Nishimura, V. Gray, J. R. Allardice, Z. Zhang, A. Pershin, D. Beljonne, A. Rao, *ACS Mater. Lett.* **2019**, *1*, 660–664.
- [73] K. J. Fallon, E. M. Churchill, S. N. Sanders, J. Shee, J. L. Weber, R. Meir, S. Jockusch, D. R. Reichman, M. Y. Sfeir, D. N. Congreve, L. M. Campos, *J. Am. Chem. Soc.* **2020**, *142*, 19917–19925.
- [74] A. Maliakal, K. Raghavachari, H. Katz, E. Chandross, T. Siegrist, *Chem. Mater.* **2004**, *16*, 4980–4986.
- [75] G. Mallocci, G. Cappellini, G. Mulas, A. Mattoni, *Thin Solid Films* **2013**, *543*, 32–34.
- [76] S. J. Strickler, R. A. Berg, *J. Chem. Phys.* **1962**, *37*, 814–822.
- [77] J. Mohanty, W. M. Nau, *Photochem. Photobiol. Sci.* **2004**, *3*, 1026.

- [78] M.-S. Bertrams, C. Kerzig, *Chem. Commun.* **2021**, 57, 6752–6755.
- [79] M. Luria, M. Ofran, G. Stein, *J. Phys. Chem.* **1974**, 78, 1904–1909.
- [80] W. R. Dawson, M. W. Windsor, *J. Phys. Chem.* **1968**, 72, 3251–3260.
- [81] S. He, Y. Han, J. Guo, K. Wu, *J. Phys. Chem. Lett.* **2022**, 13, 1713–1718.
- [82] J. Isokuoortti, S. R. Allu, A. Efimov, E. Vuorimaa-Laukkanen, N. V. Tkachenko, S. A. Vinogradov, T. Laaksonen, N. A. Durandin, *J. Phys. Chem. Lett.* **2020**, 11, 318–324.
- [83] F. Strieth-Kalthoff, C. Henkel, M. Teders, A. Kahnt, W. Knolle, A. Gómez-Suárez, K. Dirian, W. Alex, K. Bergander, C. G. Daniliuc, B. Abel, D. M. Guldi, F. Glorius, *Chem* **2019**, 5, 2183–2194.
- [84] H. Uoyama, K. Goushi, K. Shizu, H. Nomura, C. Adachi, *Nature* **2012**, 492, 234–238.
- [85] M. A. Bryden, F. Millward, T. Matulaitis, D. Chen, M. Villa, A. Fermi, S. Cetin, P. Ceroni, E. Zysman-Colman, *J. Org. Chem.* **2022**, <https://doi.org/10.1021/acs.joc.2c01137>.
- [86] M. A. Bryden, E. Zysman-Colman, *Chem. Soc. Rev.* **2021**, 50, 7587–7680.
- [87] T. C. Wu, D. N. Congreve, M. A. Baldo, *Appl. Phys. Lett.* **2015**, 107, 031103.
- [88] R. Ishimatsu, S. Matsunami, K. Shizu, C. Adachi, K. Nakano, T. Imato, *J. Phys. Chem. A* **2013**, 117, 5607–5612.
- [89] D. Meroni, A. Monguzzi, F. Meinardi, *J. Chem. Phys.* **2020**, 153, 114302.
- [90] J. Perego, J. Pedrini, C. X. Bezuidenhout, P. E. Sozzani, F. Meinardi, S. Bracco, A. Comotti, A. Monguzzi, *Adv. Mater.* **2019**, 31, 1903309.
- [91] Y. Murakami, K. Kamada, *Phys. Chem. Chem. Phys.* **2021**, 23, 18268–18282.
- [92] A. Haefele, J. Blumhoff, R. S. Khnazyer, F. N. Castellano, *J. Phys. Chem. Lett.* **2012**, 3, 299–303.
- [93] Z. A. VanOrman, C. R. Conti, G. F. Strouse, L. Nienhaus, *Chem. Mater.* **2021**, 33, 452–458.
- [94] C. J. Imperiale, P. B. Green, M. Hasham, M. W. B. Wilson, *Chem. Sci.* **2021**, 12, 14111–14120.
- [95] W. Yin, T. Yu, J. Chen, R. Hu, G. Yang, Y. Zeng, Y. Li, *ACS Appl. Mater. Interfaces* **2021**, 13, 57481–57488.
- [96] R. Haruki, Y. Sasaki, K. Masutani, N. Yanai, N. Kimizuka, *Chem. Commun.* **2020**, 56, 7017–7020.
- [97] C. Fan, L. Wei, T. Niu, M. Rao, G. Cheng, J. J. Chroma, W. Wu, C. Yang, *J. Am. Chem. Soc.* **2019**, 141, 15070–15077.
- [98] Y. Wei, Y. Li, M. Zheng, X. Zhou, Y. Zou, C. Yang, *Adv. Opt. Mater.* **2020**, 8, 1902157.
- [99] Y. Wei, M. Zheng, L. Chen, X. Zhou, S. Liu, *Dalton Trans.* **2019**, 48, 11763–11771.
- [100] L. Huang, Y. Zhao, H. Zhang, K. Huang, J. Yang, G. Han, *Angew. Chem. Int. Ed.* **2017**, 56, 14400–14404; *Angew. Chem.* **2017**, 129, 14592–14596.
- [101] V. Gray in *Photochemistry* (Eds.: A. Albini, S. Protti), Royal Society of Chemistry, Cambridge, **2019**, pp. 404–420.
- [102] S. H. C. Askes, A. Bahreman, S. Bonnet, *Angew. Chem. Int. Ed.* **2014**, 53, 1029–1033; *Angew. Chem.* **2014**, 126, 1047–1051.
- [103] M. S. Meijer, V. S. Talens, M. F. Hilbers, R. E. Kieltyka, A. M. Brouwer, M. M. Natile, S. Bonnet, *Langmuir* **2019**, 35, 12079–12090.
- [104] Th. Förster, *Ann. Phys.* **1948**, 437, 55–75.
- [105] M. Montalti, A. Credi, L. Prodi, M. T. Gandolfi, *Handbook of Photochemistry*, CRC/Taylor & Francis, Boca Raton, **2006**.
- [106] M. C. Jiménez, P. Leal, M. A. Miranda, R. Tormos, *J. Chem. Soc. Chem. Commun.* **1995**, 2009–2010.
- [107] D. H. Slater, S. S. Collier, J. G. Calvert, *J. Am. Chem. Soc.* **1968**, 90, 268–273.
- [108] S. J. Peters, T. M. Blood, M. E. Kassabaum, *Eur. J. Org. Chem.* **2009**, 6104–6108.
- [109] V. Gray, A. Dreos, P. Erhart, B. Albinsson, K. Moth-Poulsen, M. Abrahamsson, *Phys. Chem. Chem. Phys.* **2017**, 19, 10931–10939.
- [110] C. Ye, V. Gray, J. Mårtensson, K. Börjesson, *J. Am. Chem. Soc.* **2019**, 141, 9578–9584.
- [111] D. G. Bossanyi, Y. Sasaki, S. Wang, D. Chekulaev, N. Kimizuka, N. Yanai, J. Clark, *JACS Au* **2021**, 1, 2188–2201.
- [112] L. Vaghi, F. Rizzo, J. Pedrini, A. Mauri, F. Meinardi, U. Cosentino, C. Greco, A. Monguzzi, A. Papagni, *Photochem. Photobiol. Sci.* **2022**, 21, 913–921.
- [113] Y. Zhang, Y. Niu, Y. Guo, J. Wang, Y. Zhang, S. Liu, X. Shen, *Angew. Chem. Int. Ed.* **2022**, 61, e202212201; *Angew. Chem.* **2022**, 134, e202212201.
- [114] M. R. Schreier, X. Guo, B. Pfund, Y. Okamoto, T. R. Ward, C. Kerzig, O. S. Wenger, *Acc. Chem. Res.* **2022**, 55, 1290–1300.
- [115] E. A. Martynova, V. A. Voloshkin, S. G. Guillet, F. Bru, M. Beliš, K. Van Hecke, C. S. J. Cazin, S. P. Nolan, *Chem. Sci.* **2022**, 13, 6852–6857.
- [116] T. O. Paulisch, L. A. Mai, F. Strieth-Kalthoff, M. J. James, C. Henkel, D. M. Guldi, F. Glorius, *Angew. Chem. Int. Ed.* **2022**, 61, e202112695; *Angew. Chem.* **2022**, 134, e202112695.

Manuscript received: October 18, 2022

Accepted manuscript online: November 18, 2022

Version of record online: January 16, 2023